Room-temperature dissociative hydrogen chemisorption on boron-doped fullerenes

Hoonkyung Lee,[1] Jia Li,[2] Gang Zhou,[2] Wenhui Duan,[2] Gunn Kim,[3] and Jisoon Ihm[1,*]

[1]*Department of Physics and Astronomy, and Center for Theoretical Physics, Seoul National University, Seoul 151-747, Republic of Korea*
[2]*Department of Physics, Tsinghua University, Beijing 100084, People's Republic of China*
[3]*BK21 Physics Research Division and Institute of Basic Science, Sungkyunkwan University, Suwon 440-746, Republic of Korea*

Using first-principles electronic structure calculations, we show that trapping-mediated dissociative chemisorption of H_2 molecules may occur on boron-doped fullerenes. Employing the Polanyi–Wigner equation and the van't Hoff–Arrhenius law parameterized by the results of first-principles calculations, we find that a H_2 molecule adsorbed on boron-doped fullerenes can be dissociated without additional catalysts. The dissociation occurs in ~0.5 ps at room temperature, which is also supported by independent molecular dynamics simulations. Our findings indicate that boron-doped fullerenes can be used as an atomic hydrogen storage material, but not a molecular hydrogen one, at ambient conditions.

PACS number(s): 68.43.Bc, 71.15.Nc

I. INTRODUCTION

In recent years, a great deal of efforts have been devoted to finding efficient hydrogen storage media for fuel-cell powered vehicles. Because of high thermal and chemical stability (i.e., good reversibility) as well as a large surface area and light mass (high gravimetric storage capacity), carbon-based nanomaterials such as fullerenes, carbon nanotubes (CNTs), graphene, and nanocrystalline graphite have received considerable attention as one of the most significant candidates for hydrogen storage materials.[1–9]

In carbon-based nanomaterials, there are two different storage states of hydrogen species. One is physisorbed H_2 molecules and the other is chemisorbed hydrogen atoms by hydrogenation. In the usual physical methods such as compression, an extremely high pressure is required to approach the U.S. Department of Energy (DOE) target of hydrogen storage (6 wt % by the year of 2010 and 9 wt % by 2015).[10] On the other hand, many theoretical studies have claimed that the carbon-based nanomaterials can store a large amount of hydrogen in the chemisorbed form.[11,12] Experimentally, it has been observed that such chemical hydrogen storage is mainly based on dissociative adsorption of H_2 molecules on carbon-based nanomaterials with the help of topological defects, high pressure,[5–7] or hydrogenation of carbon-based nanomaterials with atomic hydrogen.[8,9] In particular, the experiment of Nikitin *et al.*[8] revealed that, in the atomic hydrogen environment, CNTs are hydrogenated with the atomic coverage of up to 65%, and the hydrogenation-dehydrogenation process is reversible by heating to 650 °C. They even reported a coverage of almost 100% at the diameter of 2 nm, which corresponds to the storage capacity of ~7 wt %.[12] These results strongly suggest the possibility of hydrogen storage in carbon-based nanomaterials. However, the need for high pressure and temperature (50 MPa and 570 K), atomic hydrogen beam, or hydrogen plasma may be major obstacles for practical applications. Recently, theoretical calculations of Kim *et al.*[13] predicted that the doping of boron (B) or beryllium (Be) onto fullerenes could significantly enhance H_2 molecular binding. The calculated binding energies of 0.2–0.6 eV/H_2 to the doped fullerene and the observed barrierless H_2 absorption reveal that such lightweight carbon-based nanomaterials could be ideal for room-temperature reversible hydrogen storage media. More importantly, *B*-doped fullerenes such as $C_{54}B_6$, $C_{59}B$, and $C_{58}B_2$ have been successfully synthesized by many research groups.[11,13,14]

In this paper, using first-principles calculations, we studied the possible storage states of hydrogen species in *B*-doped fullerenes (i.e., $C_{54}B_6$), and found that the state of molecular adsorption is about 0.47 eV higher in energy than that of dissociative adsorption. The time evolution of adsorbed hydrogen species was elucidated by molecular dynamics (MD) simulations. Moreover, employing the Polanyi–Wigner equation and the van't Hoff–Arrhenius law parameterized by first-principles calculations, we obtained the escape time from the molecular adsorption state to the dissociative adsorption state at room temperature (~0.5 ps), which was independently confirmed by our MD simulations. Importantly, we demonstrated hydrogenation of $C_{54}B_6$ without catalysts or additional treatments (such as atomic hydrogen beam, hydrogen plasma, and high temperature) at the standard temperature and pressure (STP). This fact indicates the possibility of $C_{54}B_6$ as an atomic hydrogen storage material at near standard conditions.

II. COMPUTATIONAL DETAILS

All our calculations were carried out using Vienna *ab initio* simulation package (VASP)[15] based on the density functional theory.[16] The climbing image nudged elastic band (CI-NEB) method[17] was used to calculate the activation energy barrier. The plane-wave–based total energy minimization with the Vanderbilt ultrasoft pseudopotential was employed with the local density approximation (LDA) of the Ceperley–Alder (CA) form.[18–20] It is noted that for the *B*-doped carbon systems, the calculation for the H_2 adsorption with the LDA exchange-correlation functional is better than that with the generalized gradient approximation (GGA) functional, as shown by diffusion quantum Monte Carlo calculations.[13] Supercell calculations were employed throughout where the adjacent molecules are separated by over 10 Å and the kinetic
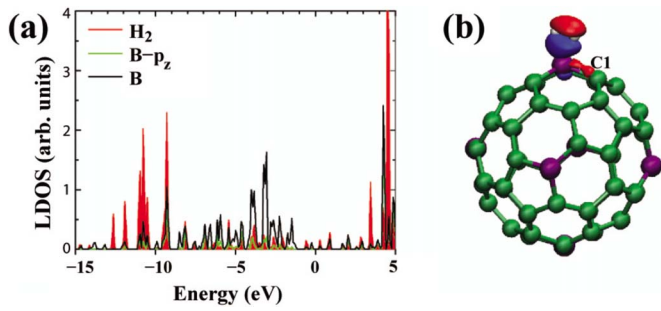
FIG. 1. (Color online) (a) Local density of states of H_2 (red line) and B (black line), and the projected density of states of B for the p_z orbital (green line) in H_2-adsorbed $C_{54}B_6$. (b) The isosurface of the electron density difference between the total system and the sum of $C_{54}B_6$ and hydrogen subsystems is shown (± 0.05 $e/Å^3$). The blue and red lobes mean electron accumulation and depletion, respectively. Green, purple, and white dots indicate carbon, boron, and hydrogen atoms, respectively.

energy cutoff was set to 287 eV. The optimized atomic positions were relaxed until the Hellmann–Feynmann force became less than 0.01 eV/Å. The Nose algorithm was employed in the MD simulation.

III. RESULTS AND DISCUSSION

We substituted six B atoms for the identical number of C atoms of C_{60}, and constructed the *B*-doped fullerene ($C_{54}B_6$) with the symmetry of D_{3d}. Our calculations showed that this configuration of $C_{54}B_6$ has lower total energy than the isomer with the symmetry of S_6 as referred to by Kim *et al.*[13] The total energy difference between them is about 0.68 eV. When $C_{54}B_6$ is synthesized at high temperature, it is in the gas phase in general,[14] so that these two configurations may coexist experimentally. We tested the stability of $C_{54}B_6$ with the D_{3d} symmetry using molecular dynamics simulations. The molecular dynamics simulation is performed within the total steps of 6000 with each time step of 0.4 fs. We heated $C_{54}B_6$ up to 1000 K for 3000 steps using a linear scaling scheme and after that, the other steps of 3000 using the Nose

algorithm at 1000 K were carried out. We found that our $C_{54}B_6$ structure is stable throughout the simulation.

In what follows, we focus on the hydrogen adsorption on the $C_{54}B_6$ with the D_{3d} symmetry, which is the most stable among configurations we tested. The previous study demonstrated that H_2 molecules are difficult to be firmly adsorbed on the pristine fullerene, due to the weakness of the van der Waals interaction between them ($\sim$tens of meV).[13] However, here we found that a single H_2 molecule can be nondissociatively adsorbed on the B site of $C_{54}B_6$ with the binding energy of 0.46 eV without an activation barrier. The distance between B and two H atoms is 1.37 Å, which is slightly smaller than that of H_2-adsorbed $C_{35}B$ (1.40 Å).[13] The local density of states (LDOS) shows the interaction between adsorbed H_2 and $C_{54}B_6$ is mainly attributed to the hybridization of the occupied σ orbital of H_2 with the localized empty p_z orbital of B of fullerene [see Fig. 1(a)], resulting in a partial charge transfer from H_2 to $C_{54}B_6$. A similar phenomenon was observed in H_2-adsorbed $C_{35}B$.[13] On the other hand, as revealed in the charge density difference in Fig. 1(b), the bonding between the B and the nearest neighbor carbon atom (C1) is obviously weakened by the H_2 adsorption. In addition, the loss of electrons in the bonding orbital of H_2 indicates that such an adsorbed H_2 molecule might no longer be stable. Typically, the bond length of the H_2 molecule is elongated to 0.87 Å from 0.75 Å upon adsorption.

The above results and analyses imply that we should go on to study dissociative adsorption of the H_2 molecule on a *B*-doped fullerene for the full understanding of the hydrogen storage mechanism. We artificially separated H_2 into two H atoms and placed them on the B site and its nearest C1 site of $C_{54}B_6$, respectively. After relaxation, this structure arrived at a stable state, as shown in Fig. 2(e), which is 0.47 eV lower than that of the molecular adsorption of H_2. To simulate a realistic situation, we implemented the CI-NEB calculation between the molecular adsorption and the dissociative adsorption of H_2, and obtained the minimum-energy path for the dissociation of the H_2 molecule on $C_{54}B_6$, as shown in Figs. 2(a)–2(f). In Fig. 2(f), we can observe that there are two metastable states and one stable state in the dissociation process. The structures in Figs. 2(b)–2(d) show the first transition state, second metastable state, and the second transition state, respectively.
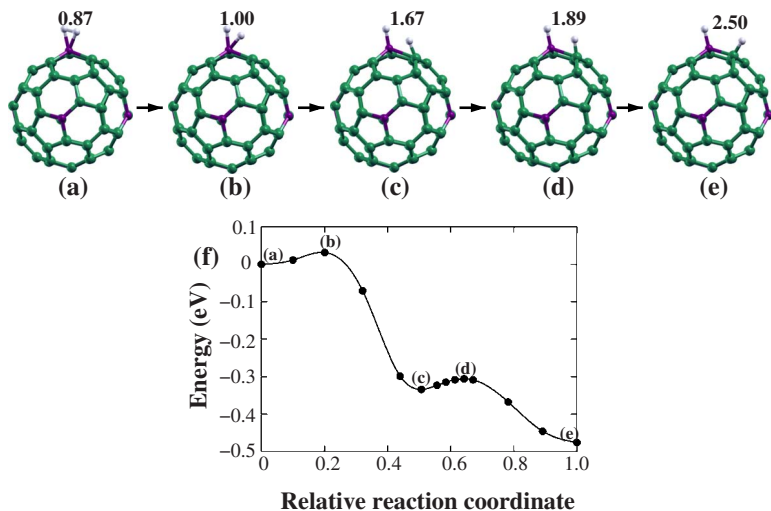

FIG. 2. (Color online) Minimum-energy path of dissociation of a H_2 molecule obtained from the CI-NEB calculation. (a)–(e) Structures corresponding to the minimum energy pathway for dissociation of the H_2 molecule obtained from the CI-NEB calculation. Numbers are the distance between the hydrogen atoms in angstrom. (f) The calculated minimum energy path of the dissociation of the H_2 molecule. Dots indicate the calculated images and the line is a smooth interpolation with the spline function. Two activation energy barriers are 32 and 28 meV, respectively, from left to right.

In the following, we calculate the escape time from the first metastable state shown in Fig. 2(a) to the stable state shown in Fig. 2(e) using the Polanyi–Wigner equation and the van't Hoff–Arrhenius law.[21,22] Adsorption coverages (θ) of hydrogen at the three states in time t are expressed by the first-order Polanyi–Wigner equation as follows:

$$\frac{d\theta_1}{dt} = -k_1\theta_1,$$

$$\frac{d\theta_2}{dt} = k_1\theta_1 - k_2\theta_2,$$

$$\frac{d\theta_3}{dt} = k_2\theta_2, \tag{1}$$

where θ_i for $i=1$, 2, and 3 represent hydrogen coverages at the first metastable state, the second metastable state, and the stable state, respectively, and k_1 (k_2) is the rate coefficient between the first metastable (the second metastable) and the second metastable state (the stable state). In Eq. (1), the reverse process from the second metastable to the first metastable state and that from the stable to the second metastable state are neglected because these backward reaction rates are vanishingly small because of too high energy barriers. At STP, the H_2 molecules fully occupy the B sites in equilibrium between adsorbed H_2 molecules and H_2 gas, because the binding energy of H_2 molecules on the $C_{54}B_6$ (= −0.46 eV) is much lower than the chemical potential of H_2 gas (=−0.32 eV).[23,24] At $t=0$, an initial coverage of θ_1 by H_2 molecules at the first metastable state is set to θ_0 (i.e., the total number of the B sites) and the initial coverages of θ_2 and θ_3 are set to zero. Then, from Eq. (1), we can obtain coverages as a function of time t:

$$\theta_1(t) = \theta_0 e^{-k_1 t},$$

$$\theta_2(t) = \frac{k_1\theta_0}{k_2 - k_1}(e^{-k_1 t} - e^{-k_2 t}),$$

$$\theta_3(t) = \frac{\theta_0}{k_2 - k_1}(k_1 e^{-k_2 t} - k_2 e^{-k_1 t} + k_2 - k_1). \tag{2}$$

The rate coefficient k_i ($i=1$ or 2) is expressed with the van't Hoff–Arrhenius law in the harmonic approximation[25]

$$k_i = \frac{\prod_{j=1}^{3N} \nu_{ij}^{IS}}{\prod_{j=1}^{3N-1} \nu_{ij}^{TS}} e^{-E_a^i/k_B T}, \tag{3}$$

where ν_{ij}^{IS} and ν_{ij}^{TS} are the frequencies of eigenmodes at the initial and transition state, respectively. E_a^i is the activation energy at each transition state, and k_B, T, and N are the Boltzmann constant, temperature, and the number of atoms, respectively. k_1 and k_2 are calculated using the van't Hoff–Arrhenius law with E_a^1 and E_a^2 being 32 and 28 meV, respectively. The frequencies of ν_{1j}^{IS} (ν_{2j}^{IS}) and ν_{1j}^{TS} (ν_{2j}^{TS}) of the states are obtained from the phonon calculations at each configuration shown in Figs. 2(a)–2(d), respectively.
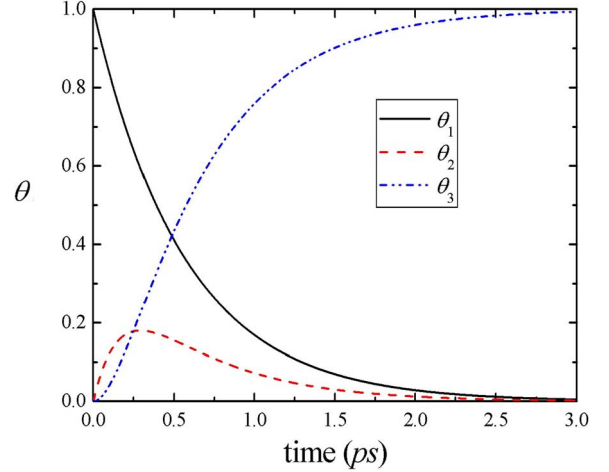

FIG. 3. (Color online) The relative hydrogen coverages at the first metastable state (θ_1), the second metastable state (θ_2), and the stable state (θ_3) as a function of time after nondissociative adsorption of H_2 molecule to $C_{54}B_6$ at 300 K.

With these formulas and the activation energies obtained from the CI-NEB calculation, θ_1, θ_2, and θ_3 at 300 K are plotted as a function of time in Fig. 3. We can see that the relative magnitude and the width of θ_2 are very small, which means that the staying time at the second metastable state is very short. This is ascribed to the fact that k_2 (=5.89 THz) is larger than k_1 (=1.78 THz), and the second metastable state hardly affects the whole process. After 0.5 ps, θ_3 sharply increases and becomes dominant. Therefore, the escape time from the first metastable state to the stable state is estimated to be ~0.5 ps.

Furthermore, we have performed MD simulations to elucidate the evolvement of adsorbed hydrogen species in time and identify the escape time from molecular adsorption to dissociative adsorption again. We have employed the time step of 0.4 fs and the temperature of 300 K in the MD simulation. Figure 4 shows the pathway for the H_2 dissociation at the time of 0.00, 0.28, 0.30, and 0.40 ps. The staying times of the first metastable and the second metastable states are 0.34 and 0.06 ps, respectively, so that the escape time in total is ~0.4 ps, which is in good agreement with the previous model calculation. Novel information obtained from the MD simulation is that the adsorbed H_2 molecule staying at the first metastable state rotates by 240° before dissociation, as shown in Fig. 4. Ultimately, the σ bond of the H_2 molecule runs parallel to the bond of B-C1, and the number-2 hydrogen atom in the figure is closer to the C1 atom. Once the H_2 molecule is dissociated, the number-2 H atom is favorably adsorbed on the C1 site, and finally accomplishes hydrogenation of $C_{54}B_6$.

We have also performed the calculations for the dissociative and nondissociative adsorption of H_2 molecules as the number of H_2 molecules increases. The binding energies for the consecutive adsorption of H_2 and the optimized structures for the nondissociative and dissociative adsorption of six H_2 molecules are shown in Figs. 5(a)–5(c). The decrease of the binding energy for the molecular adsorption is in agreement with Kim *et al.*'s[13] results, but the binding energy
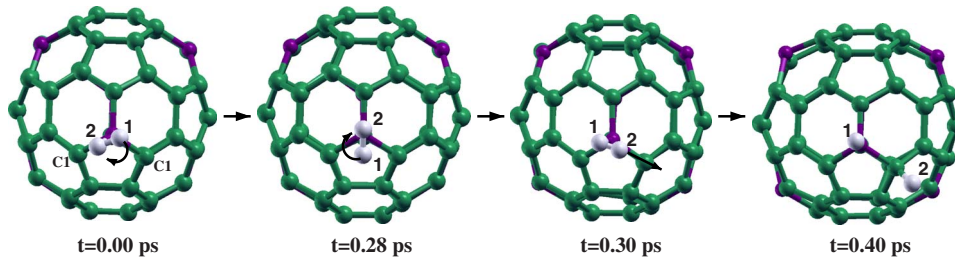
FIG. 4. (Color online) H_2 dissociation pathway on $C_{54}B_6$ obtained from molecular dynamics simulations at 0.00, 0.28, 0.30, and 0.40 ps. The numbers of 1 and 2 distinguish two hydrogen atoms. Arrows inside the fullerenes are the direction of movement of the H_2 molecule.

in $C_{54}B_6$ with the D_{3d} symmetry decreases somewhat less than that with the S_6 symmetry. It seems that the binding energy of the H_2 molecules tends to depend on different isomers. To identify whether the dissociation occurs in other isomers, we have carried out the NEB calculations between the molecular adsorption and the dissociated adsorption of H_2 molecules in isomers of S_6 and C_1 symmetries. The activation barriers are calculated to be almost the same as the results above. Therefore, the dissociation of H_2 molecules is expected to occur in all $C_{54}B_6$ molecules.

The present study has revealed that the molecular hydrogen storage state in *B*-doped fullerenes proposed by Kim *et al.*[13] is unstable in a longer time scale, and the adsorbed H_2 molecules become dissociative in ~0.5 ps. Eventually, the *B*-doped fullerene is a hydride storage material, rather than the H_2 storage one. In searching for hydrogen storage, nanomaterials such as the *B*- and *Be*-doped fullerenes as well as transition metal-decorated nanostructured materials, dissociation or nondissociation of the adsorbed H_2 molecule should be taken into account to identify the true and ultimately stable hydrogen storage state.[13,23,24,26,27]

For the purpose of comparison, we also calculated the binding energy of the H_2 molecule on the B site of *B*-doped (5,5) single-walled carbon nanotube (SWCNT), and found that it is only 0.07 eV, which is consistent with Durgun's result for the (8,0) SWCNT[28] and considerably smaller than that for the *B*-doped fullerene. Therefore, we must conclude that the interaction of the H_2 molecule with the *B*-doped fullerene is significantly different from that with the *B*-doped

SWCNT. It agrees with the recent result of Liu *et al.*[29] where they did not observe the enhanced boron-hydrogen interaction expected in *B*-doped fullerenes.[13] We suggest that the difference in the *B*-H_2 interaction between the case of *B*-doped CNTs and that of *B*-doped fullerenes might owe to different properties of *B*-induced localized states in the background structure, namely, the *B*-related state is more localized in fullerenes than in CNTs and thus interacts more strongly with H_2.

IV. SUMMARY

In summary, we have performed first-principles and model calculations for trapping-mediated dissociative chemisorption of the H_2 molecule on *B*-doped fullerenes. Using the Polanyi–Wigner equation with the van't Hoff–Arrhenius law and the MD simulation, we have found that even if a H_2 molecule is nondissociatively adsorbed on the *B*-doped fullerene initially, it becomes dissociative after ~0.5 ps at room temperature.
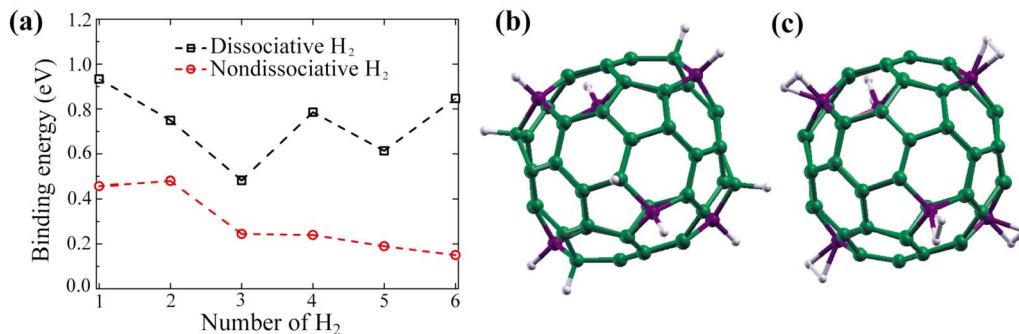
FIG. 5. (Color online) (a) Average binding energy as a function of the adsorption number of H_2 molecules. (b) Twelve H atoms adsorbed to $C_{54}B_6$. (c) Six molecular H_2 adsorbed to $C_{54}B_6$. Both structures correspond to the gravimetric density of 1.7 wt %.

*Corresponding author; jihm@snu.ac.kr

[1] S. M. Lee, K. H. An, Y. H. Lee, G. Seifert, and T. Frauenheim, J. Am. Chem. Soc. **123**, 5059 (2001).

[2] T. Yildirim, O. Gülseren, and S. Ciraci, Phys. Rev. B **64**, 075404 (2001).

[3] Y. Zhao, M. J. Heben, A. C. Dillon, L. J. Simpson, J. L. Blackburn, H. C. Dorn, and S. B. Zhang, J. Phys. Chem. C **111**, 13275 (2007).

[4] D. W. Boukhvalov, M. I. Katsnelson, and A. I. Lichtenstein, Phys. Rev. B **77**, 035427 (2008).

[5] C. Jin, R. Hettich, R. Compton, D. Joyce, J. Blencoe, and T. Burch, J. Phys. Chem. **98**, 4215 (1994).

[6] S.-P. Chan, G. Chen, X. G. Gong, and Z.-F. Liu, Phys. Rev. Lett. **87**, 205502 (2001).

[7] X. Sha and B. Jackson, J. Am. Chem. Soc. **126**, 13095 (2004).

[8] A. Nikitin, H. Ogasawara, D. Mann, R. Denecke, Z. Zhang, H. Dai, K. Cho, and A. Nilsson, Phys. Rev. Lett. **95**, 225507 (2005).

[9] G. Zhang, P. Qi, X. Wang, Y. Lu, D. Mann, X. Li, and H. Dai, J. Am. Chem. Soc. **128**, 6026 (2006).

[10] http://www.eere.energy.gov/hydrogenandfuelcells/mypp/

[11] H.-J. Muhr, R. Nesper, B. Schnyder, and R. Kötz, Chem. Phys. Lett. **249**, 399 (1996).

[12] A. Nikitin, X. Li, X. Zhang, H. Ogasawara, H. Dai, and A. Nilsson, Nano Lett. **8**, 162 (2008).

[13] Y.-H. Kim, Y. Zhao, A. Williamson, M. J. Heben, and S. B. Zhang, Phys. Rev. Lett. **96**, 016102 (2006).

[14] T. Guo, C. Jin, and R. E. Smalley, J. Phys. Chem. **95**, 4948 (1991).

[15] See http://cms.mpi.univie.ac.at/VASP.

[16] W. Kohn and L. J. Sham, Phys. Rev. **140**, A1133 (1965).

[17] G. Henkelman, B. P. Uberuaga, and H. Jonasson, J. Chem. Phys. **113**, 9901 (2000).

[18] J. Ihm, A. Zunger, and M. L. Cohen, J. Phys. C **12**, 4409 (1979).

[19] D. Vanderbilt, Phys. Rev. B **41**, 7892 (1990).

[20] D. M. Ceperley and B. J. Alder, Phys. Rev. Lett. **45**, 566 (1980).

[21] C.-H. Chung, W.-J. Jung, and I.-W. Lyo, Phys. Rev. Lett. **97**, 116102 (2006).

[22] P. Hänggi, P. Talkner, and M. Borkovec, Rev. Mod. Phys. **62**, 251 (1990).

[23] H. Lee, W. I. Choi, and J. Ihm, Phys. Rev. Lett. **97**, 056104 (2006).

[24] H. Lee, W. I. Choi, M. C. Nguyen, M.-H. Cha, E. Moon, and J. Ihm, Phys. Rev. B **76**, 195110 (2007).

[25] G. H. Vineyard, J. Phys. Chem. Solids **3**, 121 (1957).

[26] T. Yildirim and S. Ciraci, Phys. Rev. Lett. **94**, 175501 (2005).

[27] Y. Zhao, Y.-H. Kim, A. C. Dillon, M. J. Heben, and S. B. Zhang, Phys. Rev. Lett. **94**, 155504 (2005).

[28] E. Durgun, Y.-R. Jang, and S. Ciraci, Phys. Rev. B **76**, 073413 (2007).

[29] Y. Liu, C. M. Brown, J. L. Blackburn, D. A. Neumann, T. Gennett, L. Simpson, P. Parilla, A. C. Dillon, and M. J. Heben, J. Alloys Compd. **446-447**, 368 (2007).